Mon. Not. R. Astron. Soc. **000**, 000–000 (0000) Printed 2 February 2008 (MN LATEX style file v2.2)

Migration of extrasolar planets to large orbital radii

Dimitri Veras[1,2⋆] and Philip J. Armitage[1,2]
[1] *JILA, University of Colorado, 440 UCB, Boulder CO 80309-0440, USA*
[2] *Department of Astrophysical and Planetary Sciences, University of Colorado, Boulder CO 80309-0391, USA*

2 February 2008

ABSTRACT

Observations of structure in circumstellar debris discs provide circumstantial evidence for the presence of massive planets at large (several tens of AU) orbital radii, where the timescale for planet formation via core accretion is prohibitively long. Here, we investigate whether a population of distant planets can be produced via outward migration subsequent to formation in the inner disc. Two possibilities for significant outward migration are identified. First, cores that form early at radii $a \sim 10$ AU can be carried to larger radii via gravitational interaction with the gaseous disc. This process is efficient if there is strong mass loss from the disc – either within a cluster or due to photoevaporation from a star more massive than the Sun – but does not require the extremely destructive environment found, for example, in the core of the Orion Nebula. We find that, depending upon the disc model, gas disc migration can yield massive planets (several Jupiter masses) at radii of around 20-50 AU. Second, interactions within multiple planet systems can drive the outer planet into a large, normally highly eccentric orbit. A series of scattering experiments suggests that this process is most efficient for lower mass planets within systems of unequal mass ratio. This mechanism is a good candidate for explaining the origin of relatively low mass giant planets in eccentric orbits at large radii.

Key words: accretion, accretion discs — stars: formation — stars: pre-main-sequence — planetary systems: protoplanetary discs — planets and satellites: formation

1 INTRODUCTION

With one exception (Konacki et al. 2003), all confirmed extrasolar planets have been discovered by the Doppler velocity technique. The selection effects inherent to radial velocity surveys (Cumming, Marcy & Butler 1999) favor the detection of planets at small orbital radii. To date, about half of the known planets have semi-major axis $a < 1$ AU, while the most distant - 55 Cnc d - lies at 5.9 AU from its parent star. [1]. Indirect evidence, however, suggests that there could be a sizable population of massive planets at much greater radii. Recent observations of dusty debris around Vega have been interpreted as suggesting the presence of a planet of a few Jupiter masses with $a > 30$ (Wilner et al. 2002). Further, simulations modeling circumstellar dust discs suggest a planet lies at a distance of $55-65$ AU from Epsilon Eridani (Ozernoy et al. 2000).

Forming planets in these outer locations is difficult. Gas giants must form before the disc dissipates, at timescales no greater than $5 - 10$ Myr (Haisch, Lada, & Lada 2001). In standard core accretion models (Safranov 1969), the timescale for building the core of a giant planet increases rapidly with radius, with a t_{form} scaling approximately as a^2 (Pollack et al. 1996). Although such models are undoubtedly oversimplified (Pollack et al. 1996; Bryden, Lin & Ida 2000), it is hard to avoid the conclusion that forming massive planets at radii of several tens of AU within 10 Myr is difficult. Indeed, this has led to the suggestion that Uranus and Neptune may have formed at smaller radii in our own Solar System (Thommes, Duncan & Levison 1999, 2002). Motivated by these issues, we investigate the possibility of forming massive planets at small a, followed by outward migration. In Sections 2 and 3, we consider sequentially the two mechanisms that have been extensively studied in the context of inward migration: planet-disc interactions (Goldreich & Tremaine 1980; Lin & Papaloizou 1986; Lin, Bodenheimer & Richardson 1996; Trilling et al. 1998) and gravitational scattering after disc dissipation (Rasio & Ford 1996; Weidenschilling & Marzari 1996; Lin & Ida 1997; Ford, Havlickova & Rasio 2001; Terquem & Papaloizou 2002). Our conclusions are briefly summarized in Section 4.

⋆ email: Dimitri.Veras@colorado.edu

[1] From the online Extrasolar Planets Encyclopedia, at http://cfa-www.harvard.edu/planets/catalog.html (Schneider 2003) as of March 26th, 2003.

2 MIGRATION VIA GAS DISC INTERACTIONS

2.1 Methods

We calculate the orbital evolution of massive planets embedded within an evolving protoplanetary disc using a variant of the approach described by Armitage et al. (2002). We use a simple, one-dimensional (i.e. vertically averaged) treatment to model the evolution of a protoplanetary disc evolving under the action of both internal viscous torques and external torques from one or more embedded planets (Goldreich & Tremaine 1980; Lin & Papaloizou 1986; Trilling et al. 1998; Trilling, Lunine & Benz 2002). For a disc with surface density $\Sigma(R,t)$, the governing equation is,

$$\frac{\partial \Sigma}{\partial t} = \frac{1}{R}\frac{\partial}{\partial R}\left[3R^{1/2}\frac{\partial}{\partial R}\left(\nu\Sigma R^{1/2}\right) - \frac{2\Lambda\Sigma R^{3/2}}{(GM_*)^{1/2}}\right] + \dot{\Sigma}_w. \quad (1)$$

Here, ν is the kinematic viscosity which models angular momentum transport within the disc gas, and $\dot{\Sigma}_w$ is a term which allows for mass to be lost from the disc – for example as a consequence of photoevaporation. The second term within the brackets describes how the disc responds to the planetary torque, $\Lambda(R,a)$, where this function is the rate of angular momentum transfer per unit mass from the planet to the disc. For a planet in a circular orbit at radius a, we take,

$$\begin{aligned} \Lambda &= -\frac{q^2 G M_*}{2R}\left(\frac{R}{\Delta_p}\right)^4 \quad R < a \\ \Lambda &= \frac{q^2 G M_*}{2R}\left(\frac{a}{\Delta_p}\right)^4 \quad R > a \end{aligned} \quad (2)$$

where $q = M_p/M_*$, the mass ratio between the planet and the star,

$$\Delta_p = \max(H, |R-a|), \quad (3)$$

and H is the scale height of the disc. Guided by detailed protoplanetary disc models (Bell et al. 1997), we adopt $H = 0.05R$.

The transfer of angular momentum leads to orbital migration of the planet at a rate,

$$\frac{\mathrm{d}a}{\mathrm{d}t} = -\left(\frac{a}{GM_*}\right)^{1/2}\left(\frac{4\pi}{M_p}\right)\int_{R_{\rm in}}^{R_{\rm out}} R\Lambda\Sigma \mathrm{d}R, \quad (4)$$

if the only torque on the planet comes from the gravitational interaction with the disc.

In the core accretion model for giant planet formation (e.g. Pollack et al. 1996), the accretion of the gaseous envelope is predicted to take longer than any other phase of the formation process (several Myr in the baseline model for Jupiter presented by Pollack et al. 1996). In particular, the time scale for accretion is much longer than the time scale on which a sufficiently massive planet can establish a gap in the protoplanetary disc, since numerical simulations show that an approximately steady-state gap can be set up by a massive planet within $\sim 10^2$ orbital periods (e.g. Lubow, Seibert & Artymowicz 1999). A consequence of the inequality of these time scales is that massive planets – those of several Jupiter masses – probably accrete most of their envelopes *subsequent* to the development of a gap in the protoplanetary disc. Numerical simulations show how this accretion may occur. Gas from the outer disc penetrates the leaky tidal barrier created by the planet, and flows inward to form a small circumplanetary disc around the growing planet (Lubow, Seibert & Artymowicz 1999; D'Angelo, Henning & Kley 2002; Bate et al. 2003).

The existence of mass flow across gaps onto planets is intrinsically a two (or three) dimensional phenomenon (e.g. the discussion in Artymowicz & Lubow 1996). The torque function (Eq. 2) used in our one dimensional code establishes a clean gap for all planet masses above about $0.1M_J$, and this gap precludes any mass flow across the gap, or onto the planet. To allow for the mass growth of planets, we have therefore modified the one dimensional treatment to explicitly include mass flow from the outer disc on to the planet. We begin by making an approximate fit to the results of two-dimensional numerical simulations (Lubow et al. 1999; D'Angelo et al. 2002). We define the *efficiency* of mass accretion across the gap via a parameter ϵ, which is the planetary accretion rate as a fraction of the disc accretion rate at large radii (away from the location of the planet). The results of the aforementioned numerical simulations can then be approximated by the formula,

$$\frac{\epsilon}{\epsilon_{\rm max}} \simeq 1.668\left(\frac{M_p}{M_J}\right)^{1/3} e^{-\frac{M_p}{1.5M_J}} + 0.04, \quad (5)$$

where M_J is the mass of Jupiter and $\epsilon_{\rm max}$ is an adjustable parameter which can be used to test how the results depend upon the overall efficiency of planetary accretion. We use the above equation to calculate at each timestep the appropriate planetary accretion rate. We then remove the required amount of mass from the first zone on the outer edge of the gap, and add it to the mass of the planet. Note that we assume that all the mass flow onto the planet originates from the outer disc, and do not permit any material to 'bypass' the planet and flow directly from the outer disc to the inner disc.

Mass accretion across the gap onto a planet may also be expected to lead to accretion of angular momentum, given that the specific angular momentum of gas at the outer gap edge exceeds that of the planet. This effect – which it is easy to show can have a significant influence on the migration rate – cannot be straightforwardly measured from existing numerical simulations[2]. For this paper, we adopt the simplest approach, and assume that the accreted gas has the same specific angular momentum as gas at a radius $R_{gap} = 1.6a$. This fixed radius approximates the location of the outer edge of the gap throughout most of the calculation.

Eq. (1) is solved on a fixed, non-uniform mesh using standard explicit numerical methods (e.g. Pringle, Verbunt & Wade 1986). The mesh is uniform in a scaled variable $X \propto \sqrt{R}$. Typically, 300 grid points are used, with an inner boundary at 0.1 AU and an outer boundary at 200 AU. A zero-torque ($\Sigma = 0$) boundary condition is applied at R_{in}. For the protoplanetary disc model adopted, the outer boundary is at sufficiently large radius that the choice of boundary condition there has no influence on the results.

[2] Bate et al. (2003), for example, explicitly exclude this advective torque from their estimates of the migration rate, due to difficulties in measuring the net torque from the small scale circumplanetary disc formed in their simulations.

2.2 Protoplanetary disc model

We model the protoplanetary disc as a viscous accretion disc (Lynden-Bell & Pringle 1974) suffering mass loss at large radius as a consequence of photoevaporation (e.g. Shu, Johnstone & Hollenbach 1993). Motivation for considering models of this form is provided first and foremost by observations of photoevaporative flows in Orion (Johnstone, Hollenbach & Bally 1998), and is discussed further by Clarke, Gendrin & Sotomayor (2001), Matsuyama, Johnstone & Hartmann (2003), and Armitage, Clarke & Palla (2003). Briefly, we write the viscosity as a fixed (in time) power-law in radius. For most of the calculations we have adopted the form,

$$\nu = 3 \times 10^{13} \left(\frac{R}{1 \text{ AU}} \right) \text{ cm}^2 \text{ s}^{-1}. \quad (6)$$

This yields a steady-state surface density profile $\Sigma \propto R^{-1}$, which is similar to that derived from more detailed protoplanetary disc models over the radii of interest (Bell et al. 1997). To test how sensitive the conclusions are to this assumption, we have also run one model with a different form for the viscosity,

$$\nu = 1.3 \times 10^{13} \left(\frac{R}{1 \text{ AU}} \right)^{3/2} \text{ cm}^2 \text{ s}^{-1}. \quad (7)$$

Mass loss from the disc scales with radius as,

$$\begin{aligned} \dot{\Sigma}_w &= 0, \quad R < R_g \\ \dot{\Sigma}_w &\propto R^{-1}, \quad R > R_g, \end{aligned} \quad (8)$$

with $R_g = 5$ AU. We express the normalization of the mass loss via a parameter $\dot{M}_{\rm wind}$, which is defined as the total mass loss from the disc for a disc with an outer edge at 25 AU. The instantaneous rate of mass loss will therefore differ from this value depending upon the extent of the disc.

The initial surface density profile for the $\nu \propto R$ disc model is,

$$\Sigma = \Sigma_0 \left(1 - \sqrt{\frac{R_{in}}{R}} \right) \frac{1}{R} e^{-R/R_0}, \quad (9)$$

while the $\nu \propto R^{3/2}$ model is identical except for the replacement of $1/R$ by $1/R^{3/2}$. Here, Σ_0 is a constant used to define the initial accretion rate, while R_0 is a truncation radius which sets a smooth exponential cut off to the surface density at large radius. For $R \ll R_0$, a disc described by this initial condition has a constant accretion rate, so we specify the initial surface density of our models via this inner accretion rate $\dot{M}_{\rm init}$.

2.3 Results

Fig. 1 shows how the evolution of the accretion rate and disc mass varies with the strength of photoevaporative mass loss. We have computed models with our standard viscosity ($\nu \propto R$) that have $\dot{M}_{\rm wind} = 10^{-9}$ $M_\odot \text{yr}^{-1}$, $\dot{M}_{\rm wind} = 2.5 \times 10^{-9}$ $M_\odot \text{yr}^{-1}$, and $\dot{M}_{\rm wind} = 5 \times 10^{-9}$ $M_\odot \text{yr}^{-1}$. For consistency with observational determinations of protoplanetary disc parameters in nearby star-forming regions (e.g. Gullbring et al. 1998), we adopt for all of these models an initial accretion rate of $\dot{M}_{\rm init} = 5 \times 10^{-8}$ $M_\odot \text{yr}^{-1}$, and a truncation radius of $R_0 = 10$ AU. This yields an initial disc mass of 0.066 $M_\odot$. An additional model (shown as the dashed curve in Fig. 1) was calculated with the $\nu \propto R^{3/2}$ viscosity law and a mass loss of $\dot{M}_{\rm wind} = 5 \times 10^{-9}$ $M_\odot \text{yr}^{-1}$. With identical choices of $\dot{M}_{\rm init}$ and R_0, the initial disc mass for this model was 0.067 $M_\odot$.

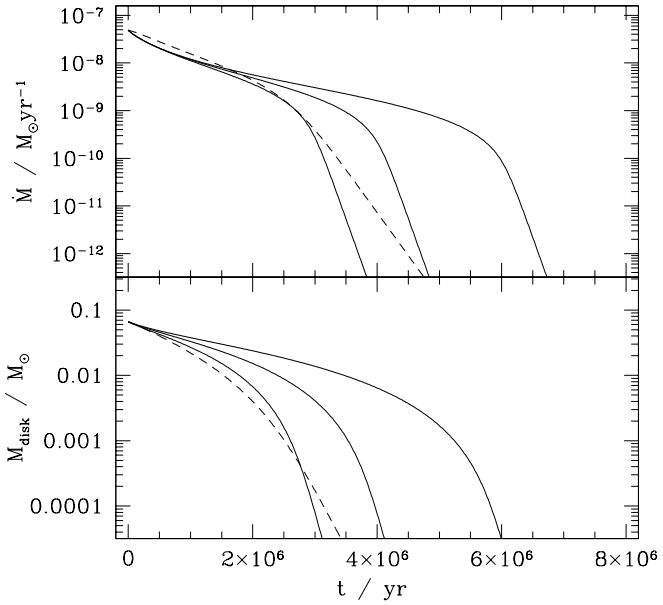

Figure 1. Evolution of the accretion rate (upper panel) and mass (lower panel) of the protoplanetary disc models used for migration calculations. The solid curves show the evolution for models with $\dot{M}_{\rm wind} = 10^{-9}$ $M_\odot \text{yr}^{-1}$, $\dot{M}_{\rm wind} = 2.5 \times 10^{-9}$ $M_\odot \text{yr}^{-1}$, and $\dot{M}_{\rm wind} = 5 \times 10^{-9}$ $M_\odot \text{yr}^{-1}$ (with increasing mass loss rates leading to smaller lifetimes). The dashed curve shows a variant model with $\nu \propto R^{3/2}$ and $\dot{M}_{\rm wind} = 5 \times 10^{-9}$ $M_\odot \text{yr}^{-1}$. The other parameters of the models are as described in the text.

As expected from previous calculations (Clarke et al. 2001; Matsuyama et al. 2003), all four models show qualitatively similar evolution. There is an initial phase in which the disc mass and accretion rate decline slowly, due primarily to mass accretion onto the star. Subsequently, the mass and accretion rate drop more rapidly as the evolution becomes dominated by mass loss via the wind (Clarke, Gendrin & Sotomayor 2001). Higher rates of mass loss reduce the disc lifetime, but all models have observationally acceptable lifetimes in the range between 4 Myr and 7 Myr. Most importantly for our purposes, in all four models mass loss is at least reasonably important (relative to accretion) for the overall evolution of the disc. The fraction of the initial disc mass that is lost in the wind varies between 40 percent and 52 percent for the $\nu \propto R$ models, and is 39 percent for the $\nu \propto R^{3/2}$ model. We note that the fraction lost in the wind is only a weak function of $\dot{M}_{\rm wind}$, because the interval of time over which the wind acts is reduced for higher instantaneous mass loss rates.

To investigate how planets migrate within the evolving disc, we run the protoplanetary disc models repeatedly. In each run, we add an initially low mass planet (0.1 M_J) into the disc at a specified time and radius. We then allow the planet to grow and migrate within the evolving disc, and record the final planet mass and orbital radius once the disc

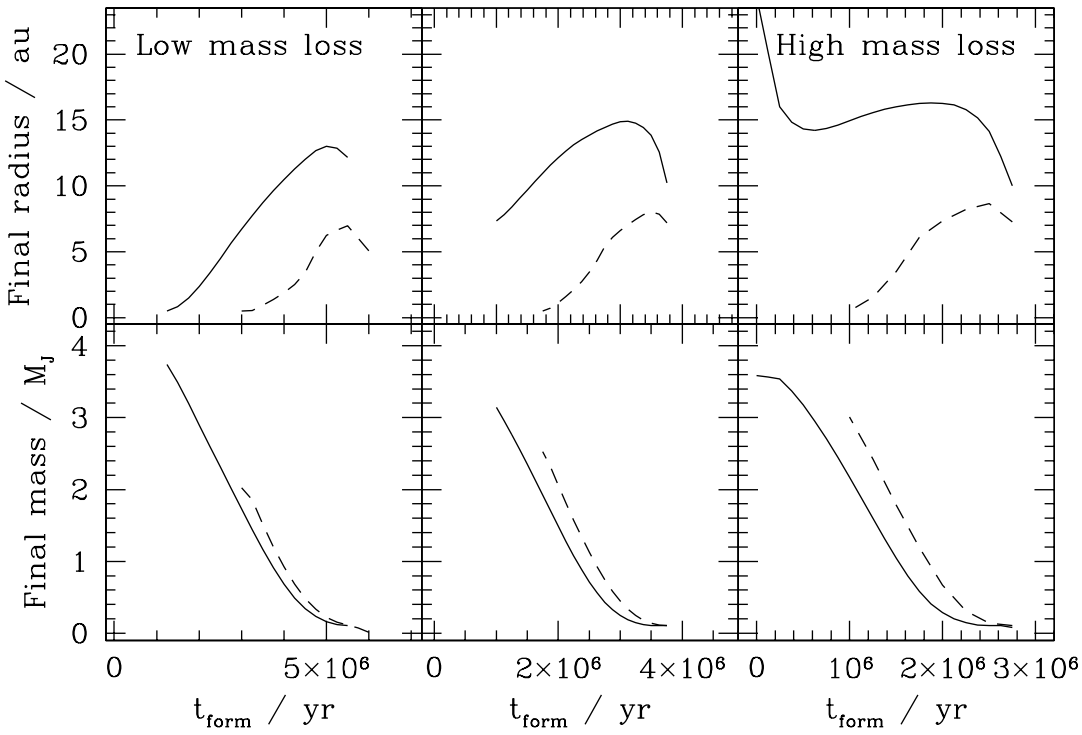

Figure 2. The final orbital radius and final mass of planets following disc migration, shown as a function of the planets' formation epoch. The dashed and solid curves show results for planets formed at initial orbital radii of 5 AU and 10 AU respectively. The left-hand panels show the extent of migration in a model disc with $\dot{M}_{\rm wind} = 10^{-9}\ M_{\odot}{\rm yr}^{-1}$, the centre panels $\dot{M}_{\rm wind} = 2.5 \times 10^{-9}\ M_{\odot}{\rm yr}^{-1}$, while the right-hand panels depict results from the $\dot{M}_{\rm wind} = 5 \times 10^{-9}\ M_{\odot}{\rm yr}^{-1}$ model.

has been either accreted or lost in the wind. By varying the formation time $t_{\rm form}$, and the formation radius $a_{\rm form}$, we study how the final outcome depends upon when and where in the disc massive planets form.

Fig. 2 shows the results for the disc with the standard viscosity law and varying rates of mass loss. We considered planet formation radii of 5 AU and 10 AU, safely outside any estimate of the snow line (Sasselov & Lecar 2000), and took $\epsilon_{\rm max} = 1$. The final planet mass and orbital radius are plotted as a function of the formation time. For the low and intermediate rates of mass loss, the sense of orbital migration is predominantly *inward*. Planets formed near the end of the disc lifetime end up in orbits close to where they formed, accrete relatively little disc gas, and remain as low mass objects. Planets formed earlier migrate inwards under the action of gravitational torques, and have time to grow to several Jupiter masses. These results are consistent with previous studies of migration (Trilling et al. 1998; Armitage et al. 2002; Trilling, Lunine & Benz 2002).

For the highest rate of mass loss from the disc, however, qualitatively different evolutionary tracks, shown in the right-hand panels of Fig. 2, are obtained. The enhanced mass loss means that there is a larger range of disc radii across which the radial velocity of the gas is outward. This can drive significant outward migration. For our choices of parameters, we find that inward migration persists for all planets formed at 5 AU, while outward migration is the rule for planets formed at 10 AU. For formation times between about 1 Myr and 2 Myr, migration approximately stalls (similar to the behaviour reported by Matsuyama, Johnstone & Murray 2003, though for slightly different reasons), while for earlier formation times the gas can drive these outer planets to radii of around 20 AU or greater. Significant accretion onto the planet occurs throughout this time, so the planets stranded at larger radii are all predicted to be massive objects.

Any attempt to distil the inherently multi-dimensional physics of planetary migration into a fast one dimensional scheme is bound to be approximate, and there are particularly obvious uncertainties in our models for planet growth and disc evolution. We have already demonstrated, as our main result, that for planets forming at radii of around 10 AU a switch between inward and outward migration occurs when $\dot{M}_{\rm wind}$ is varied by a factor of a few. The mass loss rate via photoevaporation is clearly a vital control parameter. To check how important some of the other parameters are, we have recalculated the migration of planets formed at 10 AU in two different models. In one, we altered the assumed disc viscosity (to $\nu \propto R^{3/2}$ rather than $\nu \propto R$), with the new viscosity chosen to produce a steady-state surface density profile $\Sigma \propto R^{-3/2}$. This scaling is one used often in studies of the Solar nebula (Weidenschilling 1977). A second model was computed with the standard viscosity law, but with an accretion efficiency parameter $\epsilon_{\rm max} = 0.5$. This change halves the rate of growth of planets via accretion. Both models used the high rate of mass loss previously found to be conducive to outward migration.

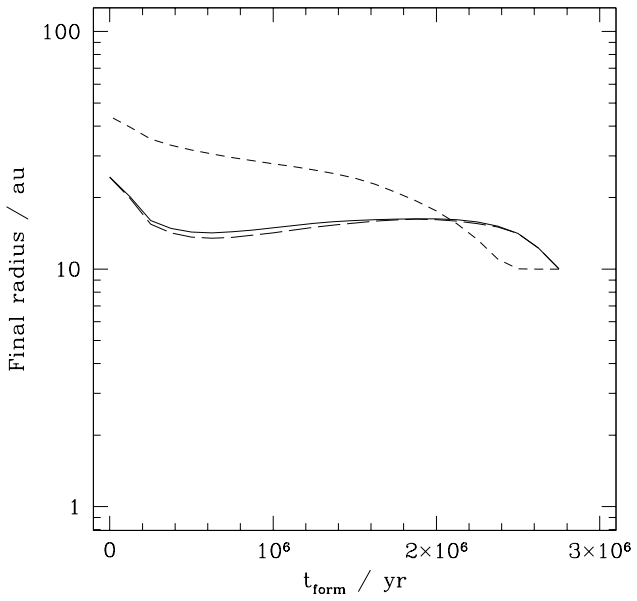

Figure 3. Sensitivity of the migration results to changes in the model parameters. The solid curve shows the extent of migration in the standard disc model with $\nu \propto R$, $\epsilon_{\rm max} = 1$, and $\dot{M}_{\rm wind} = 5 \times 10^{-9}\ M_\odot {\rm yr}^{-1}$. The short dashed curve shows a model with a different viscosity law ($\nu \propto R^{3/2}$), and the long dashed curve a model with less efficient accretion on to the planet ($\epsilon_{\rm max} = 0.5$).

Fig. 3 shows the final radii attained by planets in the three models. Outward migration occured in all three models, reflecting the primary importance of the assumed mass loss rate in determining the fates of the model planets. Changing the efficiency of accretion on to the planet made negligible difference to the final planetary radii (though it reduced the final masses of the model planets by approximately a factor of two). Substantially greater migration, however, was obtained in the calculation with the different viscosity law, despite the fact that a *smaller* fraction of the initial disc mass was actually lost to the wind in this case. We interpret this as being a side effect of the different surface density profile. Outward migration occurs when the torque from the inner disc exceeds that from the disc at radii beyond the planet's orbit. The steeper surface density profile of the $\Sigma \propto R^{-3/2}$ means that there is less mass initially exterior to the planet. As this mass is lost in the wind, the now unbalanced torque from the inner disc is more effective in driving the planet outward.

2.4 Observational implications

What are the implications of our gas disc migration calculations for the origin of planets at large orbital radii? We believe that three general conclusions can be drawn. First, mass loss from the outer disc can drive substantial outward migration, even when the mass loss is modest enough that the disc can survive for several Myr. Higher rates of mass loss would lead to more dramatic migration, but the resulting short disc lifetimes might preclude planet formation. In the central regions of the Orion Nebula, for example, Johnstone et al. (1998) infer mass loss rates between $2 \times 10^{-8}\ M_\odot {\rm yr}^{-1}$ and $6 \times 10^{-7}\ M_\odot {\rm yr}^{-1}$, with correspondingly small estimated disc lifetimes. Our results suggest that photoevaporation can have a major impact on planetary migration even in substantially more benign environments. Second, outward migration driven by the gas disc is favoured in systems where photoevaporative mass loss is stronger. The predicted rate of mass loss due to photoevaporation for a Solar mass star is rather small (Shu, Johnstone & Hollenbach 1993), so for relatively isolated stars we would expect outward migration only for stars significantly more massive than the Sun. An alternative possibility is that the mass loss is driven by external irradiation, as in the case of Orion (Johnstone, Hollenbach & Bally 1998). Finally, outward migration via this mechanism is a relatively slow process, which occurs on the viscous time of the protoplanetary disc. There is ample time for initially low mass planets to accrete substantial gaseous envelopes, so we would expect planets at large radius to be massive objects.

3 MIGRATION IN MULTIPLE PLANET SYSTEMS

3.1 Introduction

If the initial outcome of the planet formation process is a system of several massive planets, subsequent gravitational interactions can lead to many possible outcomes. Planets may collide, be ejected from the system, or settle into quasi-periodic or periodic orbits. Theoretical investigations of the orbital evolution of two-planet systems (Ford, Havlickova, & Rasio 2001) and few-planet systems (Chambers, Wetherill, & Boss 1996) have been conducted with detailed descriptions of special cases, such as equal mass planets on coplanar orbits.

Gladman (1993) established that systems with two close planets exhibit chaotic but quasi-periodic behavior given the appropriate initial conditions. Ford, Havlickova, and Rasio (2001) explored the evolution of such systems when the mass of each of two planets revolving around a solar-type star in nearly circular, coplanar orbits is equal to $10^{-3} M_\odot$. We will expand on this study by considering different mass ratios for the two planets revolving around a central star. In doing so, we will show that outward migration *is* possible, for *either* planet.

3.2 Methods

3.2.1 Motivation

The setup for our set of simulations is motivated primarily by the gravitational scattering experiments performed by Ford, Havlickova, & Rasio (2001). That study considered the interaction between two planets of mass $10^{-3} M_\odot$ (on the order of a Jupiter mass) and in an initially close configuration. The resulting branching ratios of system outcomes was explored. Systems became unstable by ejecting a planet or by a collision, one between planets or one between a planet and a star. Stable systems remained or settled into quasi-periodic orbits over 2 Myr.

The initial configuration of both planets in Ford, Havlickova, & Rasio's (2001) simulations is motivated by

μ_2 \ μ_1	1(-5)	2.5(-5)	5(-5)	7.5(-5)	1(-4)	2.5(-4)	5(-4)	7.5(-4)	1(-3)	2.5(-3)	5(-3)	7.5(-3)	1(-2)	2.5(-2)	5(-2)
1(-4)	INNER	INNER	INNER	BOTH	BOTH	OUTER	*	*	*						
5(-4)			*	*	NONE	BOTH	BOTH	*	*	NONE	NONE				
1(-3)					NONE	*	OUTER	OUTER	NONE	NONE	NONE	*	NONE		
5(-3)							NONE	NONE	NONE	*	NONE	NONE	NONE	OUTER	OUTER

Table 1. Classifying the extent of migration or lack thereof for different combinations of mass ratios, with initial parameters $0 < e_1 < 0.01$, $0 < e_2 < 0.01$, $0^\circ < i_1 < 5^\circ$, $0^\circ < i_2 < 5^\circ$, randomly chosen initial orbital angles, and initial outer semimajor axis that lies within the region of quasi-periodic orbits. "Inner" implies that the inner planet exhibited most of the outward migration, "outer" implies that the outer planet exhibited most of the outward migration, "both" implies that both planets exhibited outward migration, "none" implies neither planet exhibited significant migration, and "*" implies that $< 10\%$ of the 300 systems run were stable.

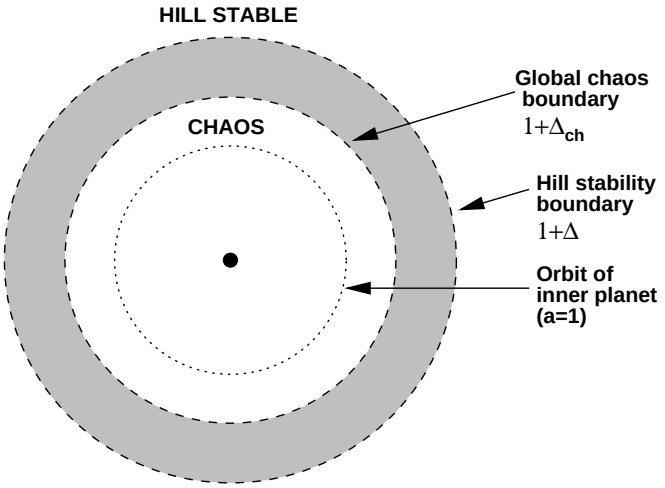

Figure 4. Schematic illustration of the initial conditions for scattering experiments. We randomly populate orbits in the shaded region, which lie outside the global chaos boundary but are inside the boundary defining guaranteed Hill stability.

the "Hill Stability Criterion", an analytic result first applied to planetary systems by Gladman (1993). A system is said to be Hill stable if the planets cannot approach each other closely for all time. We adopt Gladman's (1993) notation: Δ represents the least separation for which both planets, *for sure*, will be Hill stable. Nothing can be said about the Hill stability of a system for a separation less than Δ. Δ_{ch} represents the greatest separation at which "global chaos" will occur. A system that is "globally chaotic" might produce collisions or ejections. For a separation greater than Δ_{ch}, the planets *might* exhibit stable quasi-periodic orbits. The geometry is illustrated in Fig. 4. Gladman's (1993) analytic second order expansion for small values of μ_1 and μ_2 yields an approximate expression for Δ,

$$\Delta \simeq 2 \cdot 3^{\frac{1}{6}}(\mu_1+\mu_2)^{\frac{1}{3}} + 2 \cdot 3^{\frac{1}{6}}(\mu_1+\mu_2)^{\frac{2}{3}} - \frac{11\mu_1+7\mu_2}{3^{\frac{11}{6}}(\mu_1+\mu_2)^{\frac{1}{3}}}.$$

Unlike Δ, an approximation for Δ_{ch} can only be found empirically. By developing overlap resonance criteria for two-planet systems, Wisdom (1980) derived the following approximation when $\mu_1 = \mu_2 = \mu$:

$$\Delta_{ch} \simeq 2\mu^{\frac{2}{7}}$$

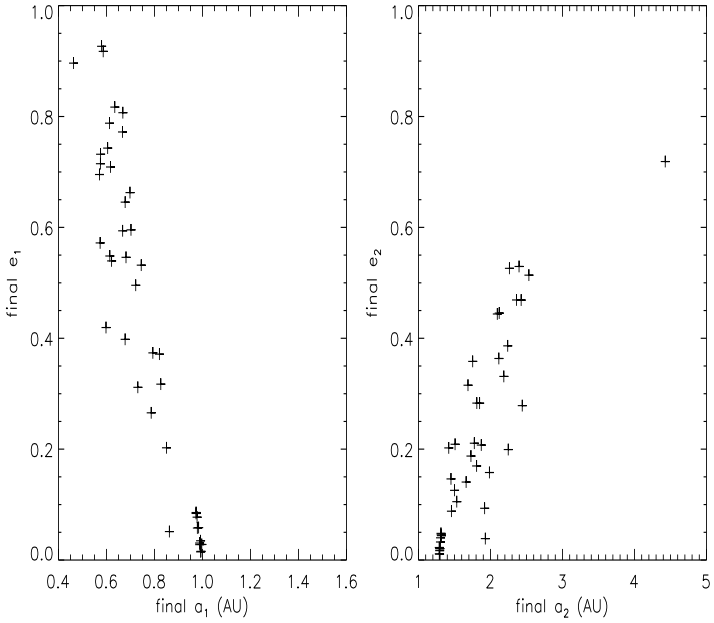

Figure 5. Scatter plots of the final eccentricity vs. semimajor axis for both planets in the stable systems where $\mu_1 = 5 \times 10^{-4}$, $\mu_2 = 1 \times 10^{-3}$.

Ford, Havlickova, & Rasio (2001) ran simulations where the initial semimajor axis separation of the planets lay between Δ and Δ_{ch}, so that the planets would neither be in a Hill Stable configuration nor become unstable immediately. In this work, we sample the entire initial separation range spanned by Δ and Δ_{ch} in order to best detect planets that may migrate outwards and remain on quasi-periodic orbits.

3.2.2 Simulation Setup

We denote the semimajor axis of the initially inner planet a_1, the initially outer planet a_2, and the respective planet mass/central mass ratios as μ_1 and μ_2. Other orbital elements will distinguish the planets with a subscript of "1" or "2". All runs were performed with $a_1 = 1$ AU, so that the results may be scaled easily to any ratio of semimajor axes, such as for $a_1 = 5 - 10$ AU.

All numerical runs of the three-body system were per-

formed with a Bulirsch-Stoer routine from the HNbody integration package (Rauch & Hamilton 2002). The routine ran for 2 Myr with an accuracy parameter of 10^{-12}, and was rerun with uniformly smaller initial timesteps when necessary until this accuracy was achieved. For each run, the Bulirsch-Stoer routine began with an initial timestep of 0.05 yr, and the orbital elements of each body were output every 0.01 Myr. In most cases, energy and angular momentum errors, expressed by $(E - E_0)/E_0$ and $(L_Z - L_{Z_0})/L_{Z_0}$, where E_0 is the initial total system energy and L_{Z_0} is the initial total angular momentum in the direction perpendicular to the orbital plane, did not exceed 10^{-7}. In the most pathological cases, energy and z-angular momentum errors were conserved to within 10^{-4}. Angular momenta in the other two directions were typically conserved to two order of magnitudes better than the z-angular momentum.

We are most interested in the evolution of stable systems in which both planets remain bound. We define stable systems as systems where both planets have semimajor axes which never exceed 10^3 AU and eccentricities which never exceed 0.99. Further, we deemed a system unstable if at any time the HNbody code outputted a negative value for the semimajor axis or eccentricity of either planet.

A preliminary exploration of phase space revealed that of the systems that become unstable, most did so within 0.05 Myr. Thus, each system underwent several checks at 0.05 Myr; unstable systems were terminated, and stable systems were evolved for a total of 2 Myr. In order to reduce computer time, we imposed additional conditions on systems after 0.05 Myr. Systems not satisfying these conditions were terminated. Given that $a_1 = 1$ AU for each run, the conditions are

1) 1.2 AU $< a_2 <$ 3.0 AU,
2) $a_1 <$ 1.05 AU,
3) If $a_2/a_1 < 1.5$, then $e_2 < 0.1$,
4) If $a_2/a_1 > 1.5$, then $e_2 < 0.3$.

These conditions were chosen based on a preliminary exploration of the properties of unstable systems. For example, we found that after 0.05 Myr, if the semimajor axis of the outer planet is within 50% of a_1, then a high (> 0.1) eccentricity of the outer planet implies that the system will become unstable.

By definition, long-term chaotic behavior may differ drastically due to an infinitesimal change in initial conditions. Therefore, because computers use finite-precision arithmetic, individual runs are largely irreproducible from machine to machine. In this context, one can only make statements about the probability of a system behaving in a certain manner (Quinlan & Tremaine 1992). Thus, for each particular dimension of phase space explored, we performed 300 runs, each with randomly chosen initial orbital parameters that lay within specific ranges.

We expanded on the results of Ford, Havlickova, and Rasio (2001) by investigating the effects of altering the planet/star mass ratio for each planet. For each pair of mass ratios, 300 runs were performed, each run with both planets having a randomly chosen initial eccentricity between 0 and 0.01 and initial inclination between 0° and 5°, along with an argument of perihelion, longitude of ascending node, and mean anomaly each randomly chosen between 0° and 360°.

We performed 9 sets of 300 runs for each of the following four outer planet mass ratios μ_2: 1×10^{-4}, 5×10^{-4}, 1×10^{-3}, and 5×10^{-3}. Each set of runs corresponds to a different inner planet mass ratio. We varied the mass of the inner planet within one order of magnitude of the mass of the outer planet. As mentioned, the initial semimajor axis of the inner planet for every run was set at 1.0 AU. The initial semimajor axis of the outer planet was chosen in a regime that exhibited unpredictable behavior but allowed for quasi-periodic orbits. Explanation of this regime follows.

As mentioned previously, the region bounded by Δ and Δ_{ch} describe systems that *may* exhibit Hill instability and *may* exhibit quasi-periodic motion. When both are exhibited, *some* planets exhibit outward migration, which is the topic of this section. So as to include all regions from which migrating behavior might arise, we took $\Delta_{ch} = 2 \cdot [min(\mu_1, \mu_2)]^{\frac{2}{7}}$. Because $a_1 = 1$ AU for each run, values of a_2 were randomly chosen between $1 + \Delta_{ch}$ and $1 + \Delta$ for the simulations.

Our initial conditions for the scattering experiments are similar to those adopted by most previous authors (e.g. Ford, Havlickova & Rasio 2001; Marzari & Weidenschilling 2002; Chambers, Wetherill & Boss 1996), in that we start with fully-formed planets in relatively close proximity to each other, and consider only their mutual gravitational interactions. Such initial conditions are chosen primarily for simplicity and compatibility with previous work, and can only partially be justified on physical grounds. In particular, since many of the trial systems prove to be unstable over time scales comparable to the lifetime of protoplanetary discs (Haisch, Lada & Lada 2001), there is likely to be an earlier epoch during which *both* planet-planet gravitational interactions and planet-disc interactions are important. This earlier stage of evolution could lead to an unstable multiple planet system in at least two ways. First, two planets might form in well-separated orbits, but then subsequently migrate into an unstable configuration as a consequence of disc-driven migration (Goldreich & Tremaine 1980; Lin & Papaloizou 1986; Lin, Bodenheimer & Richardson 1996). For this to happen, the planets would have to avoid becoming trapped into resonance during the migration process (Snellgrove, Papaloizou & Nelson 2001; Lee & Peale 2002; Murray, Paskowitz & Holman 2002). Alternatively, the planets might form close together, and be stabilized against immediate violent instability by the presence of a surrounding gas disc (Lin & Ida 1997; Nagasawa, Lin & Ida 2003)[3]. Further, unstable planetary systems may form after the disc has dissipated. Planet-planet interactions alone in crowded systems of Jovian-mass planets most often leaves only two survivors in close, quasiperiodic but ultimately unstable orbits (Adams & Laughlin 2003). Although any of these pathways could plausibly lead to initial conditions that are similar to those which we (and other authors) have assumed, a full treatment will obviously need to model the more complex interactions that are possible during the phase when the gas disc is being dispersed.

[3] In related work, Agnor & Ward (2002) considered the damping of *terrestrial* planet eccentricity by a remnant gas disc.

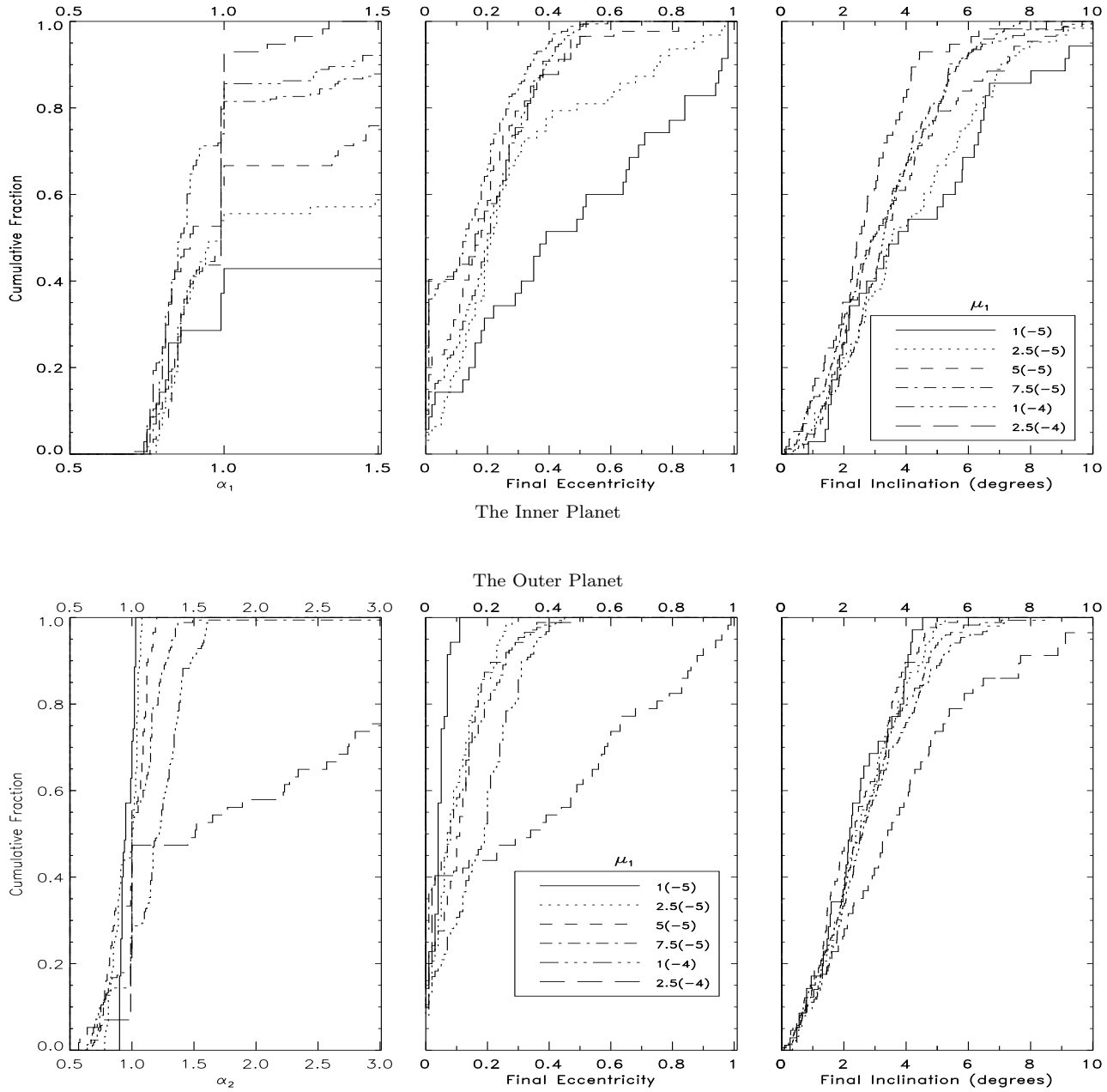

Figure 6. Cumulative probability distributions for stable systems with $\mu_2 = 1 \times 10^{-4}$. For clarity, values of μ_1 are abbreviated such that $1 \times 10^{-5} \equiv 1(-5)$. The upper panel represents orbital parameter distributions of the inner planet, and the lower panel the outer planet.

3.3 Results

Table 1 and Figs. 6-9 displays the data we took. Table 1 summarizes the data in terms of mass ratio and extent of migration, while the figures provide a more detailed look at migration behavior. Fig. 5 provides a representative sample of the final semimajor axes and eccentricities of both planets when significant outward migration occurs, and provides a perspective on how data is plotted in Figs. 6-9. For example, the 43 stable systems displayed in Fig. 5 are plotted as the solid lines in Fig. 8. Fig. 5 illustrates that planets that migrate both inward and outward tend to increase their eccentricity. Although the extent of migration in both directions is similar, those planets that migrate inward tend to increase their eccentricities at a higher rate.

Figs. 6-9 each represent a set of six cumulative probability distributions that display the fraction of *stable* systems vs. semimajor axis ratios, eccentricities, and inclinations of the outer and inner planet after exactly 2 Myr. The upper panel in each figure represents the initially outer planet, and

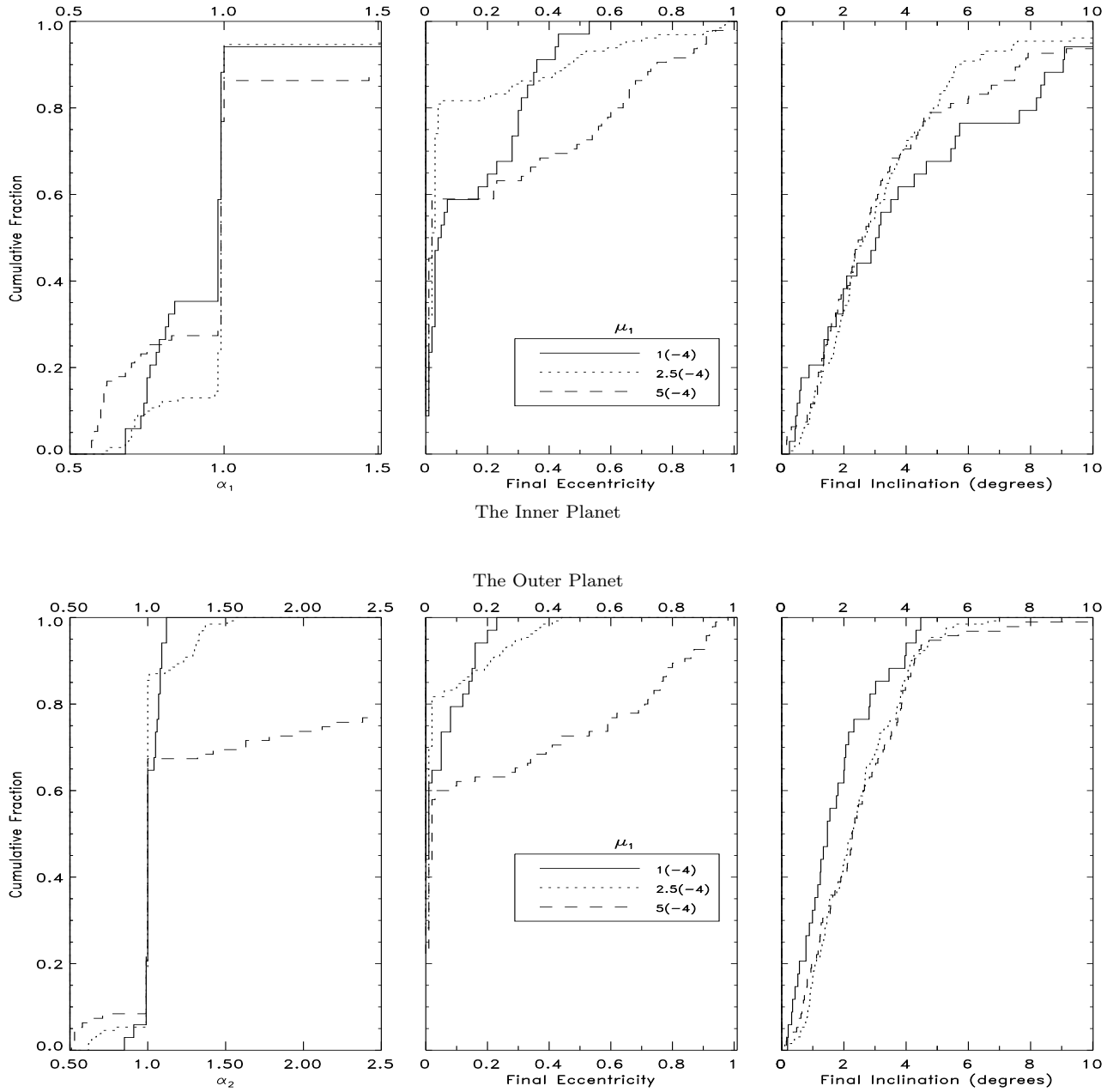

Figure 7. Cumulative probability distributions for stable systems with $\mu_2 = 5 \times 10^{-4}$. For clarity, values of μ_1 are abbreviated such that $1 \times 10^{-4} \equiv 1(-4)$. The upper panel represents orbital parameter distributions of the inner planet, and the lower panel the outer planet.

the lower panel represent the initially inner planet. Each figure keeps the mass of the outer planet fixed, but varies the mass of the inner planet. Although we obtained nine curves for each graph on each figure, we show only the curves that exhibit significant radially outward migration, plus some that do not, and we do not show any curves where less than 10% of the 300 runs were stable.

Detecting migration for the outer planets is difficult because their semimajor axes were randomly chosen for each run. To aid in determining the net radial movement of these planets, we define $\alpha_1 \equiv a_1(\text{final})/a_1(\text{initial})$ and $\alpha_2 \equiv a_2(\text{final})/a_2(\text{initial})$. Each panel in Figs. 6-9 contain distributions of semimajor axis ratios, rather than absolute semimajor axes, because those are scalable in this study.

Table 1 and Figs. 6-9 illustrate that outward migration of both the inner and outer planets occurs more frequently with smaller values of μ_2. Fig. 6 displays extensive migration. In the lowest mass case, almost 60% of the stable inner planets migrate at outward to at least 150% of their original semimajor axis. As μ_1 is increased, migration occurs less fre-

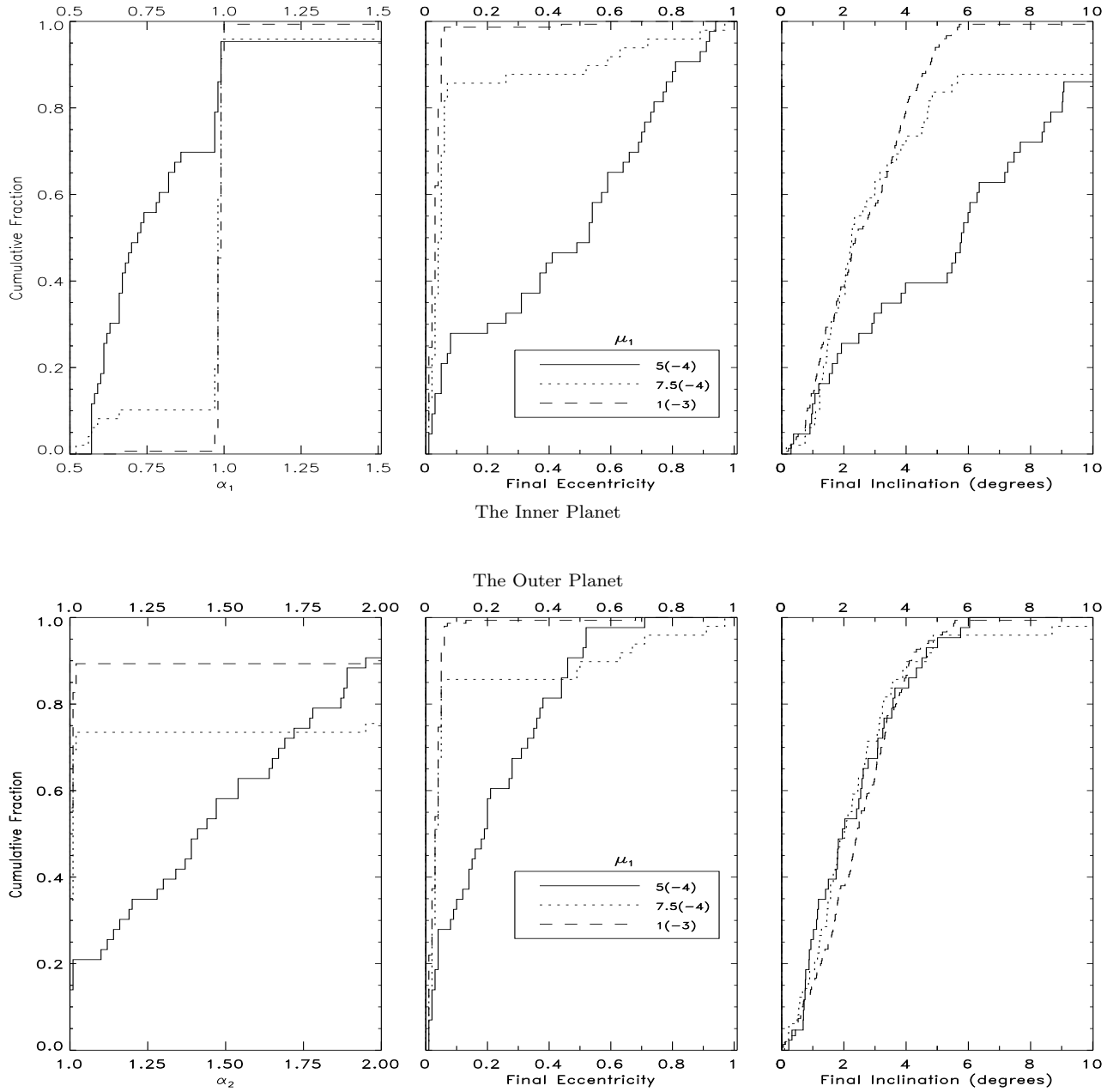

Figure 8. Cumulative probability distributions for stable systems with $\mu_2 = 1 \times 10^{-3}$. For clarity, values of μ_1 are abbreviated such that $5 \times 10^{-4} \equiv 5(-4)$. The upper panel represents orbital parameter distributions of the inner planet, and the lower panel the outer planet.

quently; for $\mu_1 = 2.5 \times 10^{-4}$ no inner planets migrated out to 150% of their original semimajor axis. The correlation of mass ratio to final state behavior is less apparent but still present in the final eccentricity and inclination curves. In both graphs, the least-mass case prompts the highest final eccentricity and inclination values for the orbit of the inner planet.

The final state of the outer planet, represented by the lower panel of Fig. 6, reflects the exchange of angular momentum in this system. One sees that when an inner planet migrates outward, it leaves the initially outward planet back so that $\alpha_2 < 1$. The one instance where the outer planet experiences significant migration is the highest mass case - the same case where $\alpha_1 < 1.5$. The eccentricity and inclination distributions for the outer planet in this massive case differ drastically from the behavior seen for other inner planet masses.

In Fig. 7, $\mu_2 = 5 \times 10^{-4}$ and the result is significantly less migration than seen in Fig. 6. Similarly to Fig. 6, the highest mass case exhibits the greatest migration of the

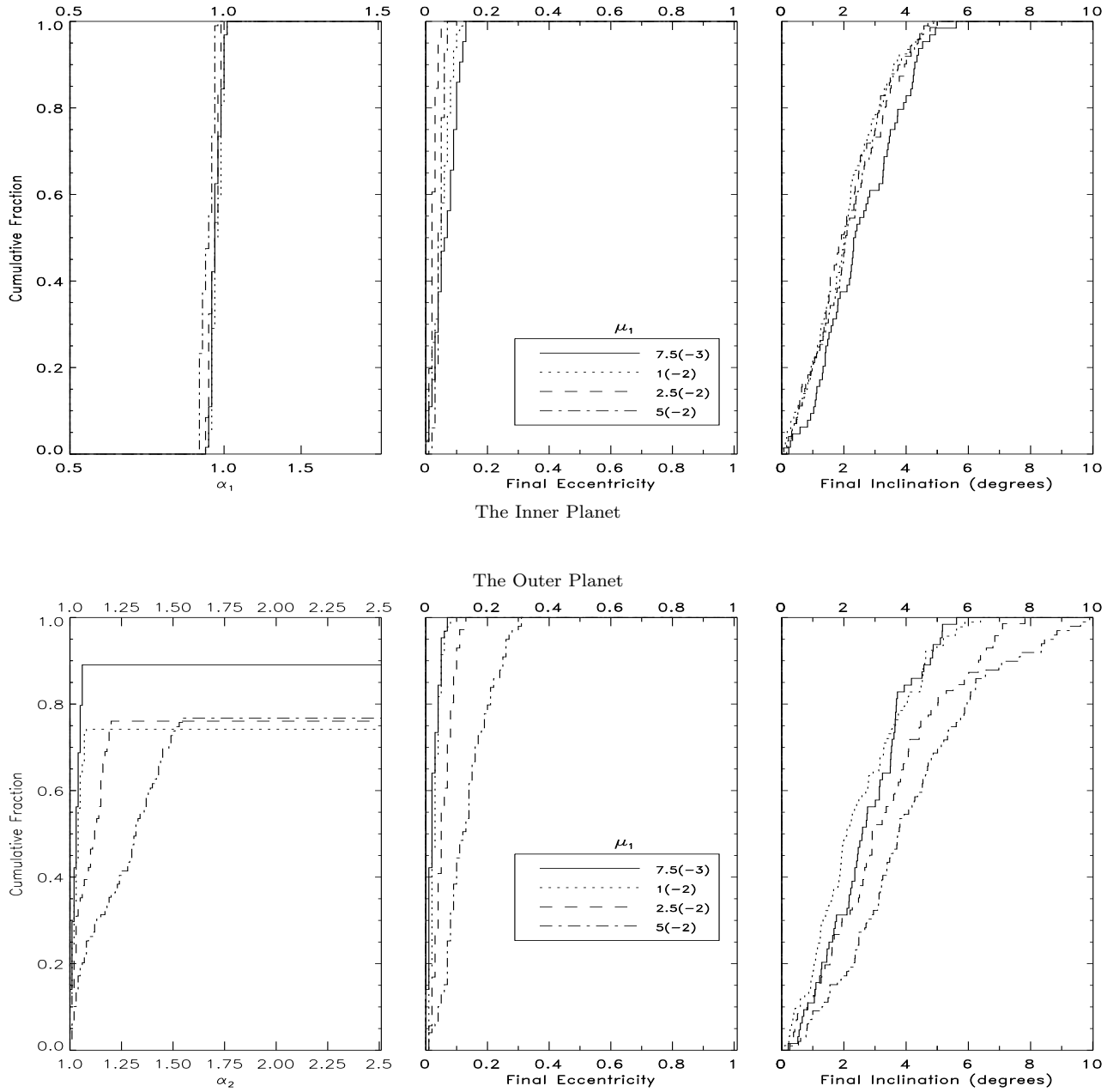

Figure 9. Cumulative probability distributions for stable systems with $\mu_2 = 5 \times 10^{-3}$. For clarity, values of μ_1 are abbreviated such that $7.5 \times 10^{-3} \equiv 7.5(-3)$. The upper panel represents orbital parameter distributions of the inner planet, and the lower panel the outer planet.

outer planet. In this case, $\simeq$20% of the outer planets and $\simeq$15% of the inner planets migrate beyond 150% of their original semimajor axis. Halving the inner mass value reduces the probability for $\alpha_1 < 1.5$ or $\alpha_2 < 1.5$ to $\simeq$5%. In contrast to Fig. 6, the least mass case fails to show significant outward migration of the inner planet, despite the inner planet exhibiting the highest final inclinations.

In Fig. 8, where the outer mass is a full order of magnitude more massive than in Fig. 6, we see even less migration. Inner bodies for the smallest mass case exhibit high eccentricities and inclinations, but only $\simeq$5% satisfy $\alpha_1 > 1.5$. The case where $\mu_1 = \mu_2 = 1 \times 10^{-3}$ is the same case studied by Ford, Havlickova, & Rasio (2001). Their Figs. 11-12 can be compared to the semimajor axis ratio distributions, eccentricity distributions, and inclination distributions in Fig. 8.

No migration of the inner planet occurs for any case in Fig. 9. However, the outer planet shows significant migration. Further, as shown by the sequence of four curves in the lower panel, the higher the mass of the outer planet,

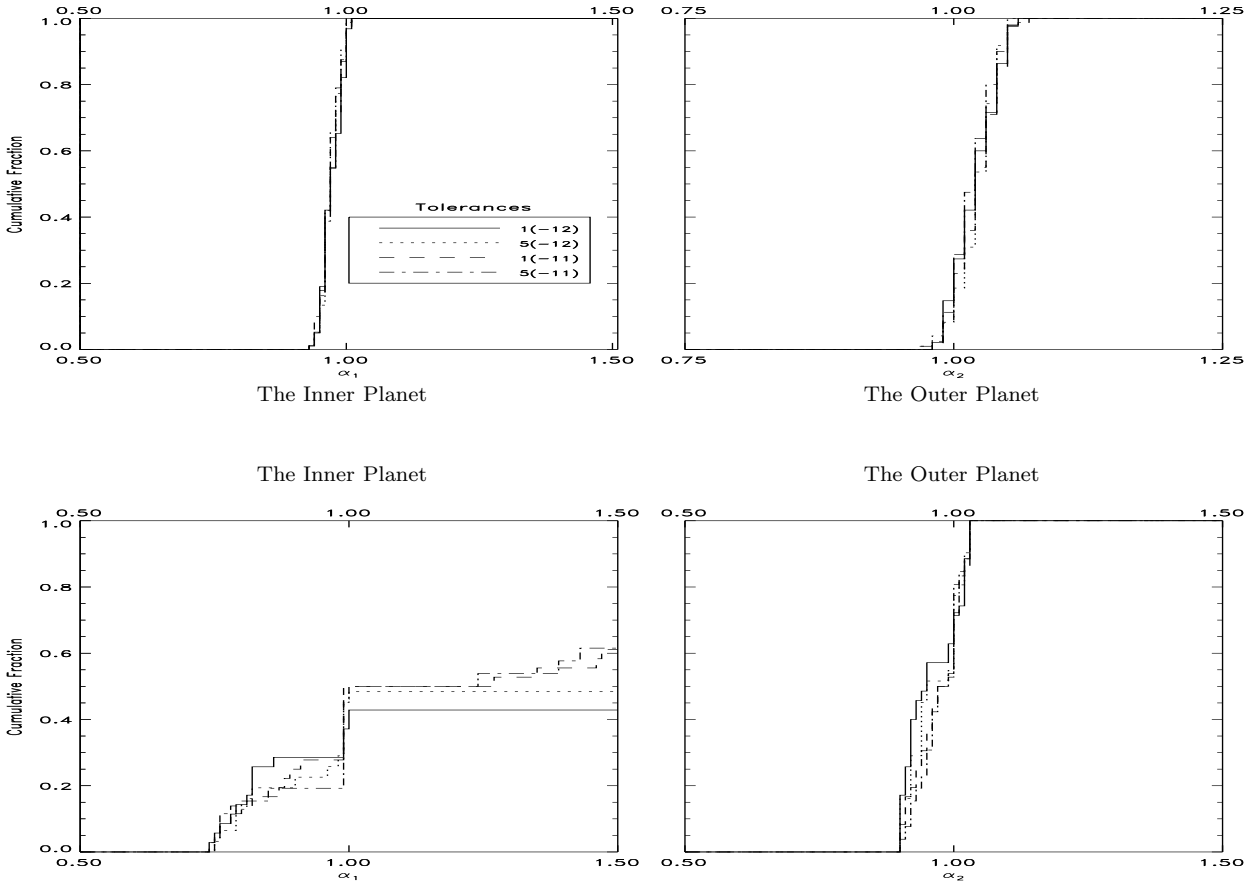

Figure 10. Cumulative probability distributions for a system with negligible migration ($\mu_1 = \mu_2 = 5 \times 10^{-3}$, upper panel) and for a system with significant migration ($\mu_1 = 1 \times 10^{-5},\ \mu_2 = 1 \times 10^{-4}$, lower panel) for different tolerances, which are given with abbreviated scientific notation. 900 runs were performed for the upper panel system, and 300 were performed for the lower panel system. Similarly to Figs. 6-9, only the stable systems are shown.

the greater the extent of the migration. For the higher mass cases, about 25% of the initally outer planets satisfy $\alpha_2 > 2.5$. Remarkably, these planets all retain final eccentricities < 0.4, in stark contrast to the large final eccentricities of the migrating planets of Figs. 6-8.

Because of the chaotic nature of the three body problem, one encounters difficulty when predicting the appropriate timescale over which to integrate. We adopted a similar timescale to the one used by Ford, Havlickova, & Rasio (2001), but recognize that systems that appear to be stable at 2 Myr might become unstable at some future time. We extended the running time of one system to sample the consequences. After 2 Myr, 55 out of the 300 systems for the case $\mu_1 = 5 \times 10^{-3},\ \mu_2 = 1 \times 10^{-3}$ remain stable. By running this system for 10 Myr, we found only 3 out of the 55 systems became unstable, and did so quickly. Further, these three systems became unstable before 3 Myr.

For any set of 300 runs of a chaotic system, the slightest change in any input parameter of the Bulirsch-Stoer algorithm might drastically alter the results of any individual runs, but keep the same global behavior. The extent of the invariance of this global behavior is a function of the code used and the number of systems sampled. To explore this measure of invariance for the runs presented here, we reran two systems with four different initial tolerances (5×10^{-11}, 1×10^{-11}, 5×10^{-12}, 1×10^{-12}). One of these systems ($\mu_1 = \mu_2 = 5 \times 10^{-3}$) exhibited negligible migration, and the other ($\mu_1 = 1 \times 10^{-5},\ \mu_2 = 1 \times 10^{-4}$) exhibited significant migration. In order to achieve the largest feasible sample size for this error analysis, we tripled the number of runs performed to 900 for the system exhibiting negligible migration. As Fig. 10 illustrates, runs with different tolerances are practically indistinguishable for the case of no migration, but vary up to 20% for the case of significant migration.

3.4 Summary

The gravitational interaction of a pair of unequal mass planets that lie in close initial configurations allow *either* planet to migrate outward to at least twice it's initial semimajor axis. Planets that migrate outward lie in quasi-stable, slightly inclined eccentric orbits with an eccentricity that spans the entire permissible range and an inclination up to about 10°. Although either planet in any given system may drift outward, the smaller the mass of the planets, the higher

the tendency for the initially inner planet to migrate outward. Further, less massive giant planets such as Uranus or Neptune are more likely to migrate outward than Jupiter-mass planets. This result, derived from our gravitational scattering simulations alone, is consistent with Thommes, Duncan & Levison's (1999, 2002) conclusion that Uranus and Neptune's current location is a result of outward migration amongst Jupiter and Saturn.

4 CONCLUSIONS

As a first step in explaining the presence of planets at large orbital radii, we have shown that outward migration of protoplanets is possible both by planet-disc interactions and by planet-planet gravitational scattering without the presence of a disc. Strong mass loss in discs coupled with planetary cores that are formed at about ~ 10 AU allow planets to migrate outward in discs to radii that are as much as a factor of several in excess of their initial semimajor axes. Planets that migrate in such a manner are likely to be massive. We predict that gas-driven outward migration should be most likely to occur around more massive stars, whose strong UV flux can drive a powerful photoevaporative outflow. Subsequently, when in the appropriate chaotic regime, planets within a multiple planet system may migrate outward due to gravitational scattering alone. Planets that migrate in this manner may be massive or not, however low mass objects tend to exhibit the most extensive outward migration. Orbital migration is typically accompanied by an increase in eccentricity that spans the allowable range for elliptic orbits.

ACKNOWLEDGMENTS

We thank an anonymous referree for helpful comments, Kevin Rauch and Doug Hamilton for use of their integrator and assistance in it's operation, as well as the Colorado Rings Group for useful discussions.

This paper is based upon work supported by NASA under Grant NAG5-13207 issued through the Office of Space Science.

REFERENCES

Adams F.C., Laughlin G., 2003, Icarus in press
Agnor C.B., Ward W.R., 2002, AAS DDA meeting #33 #07.12
Armitage P.J., Clarke C.J., Palla F., 2003, MNRAS in press
Armitage P.J., Livio M., Lubow S.H., Pringle J.E., 2002, MNRAS 334, 248
Artymowicz P., Lubow S.H., 1996, ApJ 467, L77
Bate M.R., Lubow S.H., Ogilvie G.I., Miller K.A., 2003, MNRAS in press, astro-ph/0301154
Bell K.R., Cassen P.M., Klahr H.H., Henning Th., 1997, ApJ, 486, 372
Bryden G., Lin D.N.C., Ida S., 2000, ApJ, 544, 481
Chambers J.E., Wetherill G.W., Boss A.P., 1996, Icarus 119, 261
Charbonneau D., Brown T.M., Latham D.W., Mayor M., 2000, ApJ 529, L45
Clarke C.J., Gendrin A., Sotomayor M., 2001, MNRAS 328, 485
Cumming A., Marcy G.W., Butler R.P., 1999, ApJ 526, 890
D'Angelo G., Henning T., Kley W., 2002, A&A 385, 647
Ford E.B., Havlickova M., Rasio F.A., 2001, Icarus 150, 303
Gladman B., 1993, Icarus 106, 247
Goldreich P., Tremaine S., 1980, ApJ 241, 425
Gullbring E., Hartmann L., Briceno C., Calvet N., 1998, ApJ 492, 323
Haisch K.E., Lada E.A., Lada C.J., 2001, ApJ 553, L153
Johnstone D., Hollenbach D., Bally J., 1998, ApJ 499, 758
Konacki M., Torres G., Jha S., Sasselov D., 2003, Nature 421, 507
Lee M., Peale S.J., 2002, ApJ 567, 596
Lin D.N.C., Bodenheimer P., Richardson D.C., 1996, Nature 380, 606
Lin D.N.C., Ida S., 1997, ApJ 477, 781
Lin D.N.C., Papaloizou J, 1986, ApJ 309, 846L
Lubow S.H., Seibert M., Artymowicz P., 1999, ApJ 526, 1001
Lynden-Bell D., Pringle J.E., 1974, MNRAS 168, 603
Marzari F., Weidenschilling S.J., 2002, Icarus 156, 570
Matsuyama I., Johnstone D., Hartmann L., 2003, ApJ 582, 893
Matsuyama I., Johnstone D., Murray N., 2003, ApJ 585, L143
Murray N., Paskowitz M., Holman M., 2002, ApJ 565, 608
Nagasawa M., Lin D.N.C., Ida S., 2003, ApJ 586, 1374
Ozernoy L.M., Gorkavyi N.N., Mather J.C., Taidakova T.A., 2000, 537, L147
Pollack J.B., Hubickyj O., Bodenheimer P., Lissauer J.J., Podolak M., Greenzweig Y., 1996, Icarus 124, 62
Pringle J.E., Verbunt F., Wade R.A., 1986, MNRAS 221, 169
Quinlan G.D., Tremaine S., 1992, MNRAS 259, 505
Rasio F.A., Ford E.B., 1996, Science 274, 954.
Rauch K.P., Hamilton D.P., 2002, AAS DDA meeting #33 #08.02
Safronov V.S., 1969, Evolution of the Protoplanetary Cloud and Formation of the Earth and Planets. Nauka, Moscow.
Sasselov D.D., Lecar M., 2000, ApJ 528, 995
Shu F.H., Johnstone D., Hollenbach D., 1993, Icarus 106, 92
Snellgrove M.D., Papaloizou J.C.B., Nelson R.P, 2001, A&A 374, 1092
Terquem C., Papaloizou J.C.B., 2002, MNRAS 332, L39
Thommes E.W., Duncan M.J., Levison H.F., 1999, Nature 402, 635
Thommes E.W., Duncan M.J., Levison H.F., 2002, AJ 123, 2862
Trilling D.E., et al., 1998, ApJ 500, 428
Trilling D.E., Lunine J.I., Benz W., 2002, A&A 394, 241
Weidenschilling, S.J. 1977, Ap&SS, 51, 153
Weidenschilling S.J., Marzari F., 1996, Nature 384, 619
Wilner D.J., Holman M.J., Kuchner M.J., Ho P.T.P., 2002, ApJ 569, L115